

Special  
Issue

# Novel Cofacial Porphyrin-Based Homo- and Heterotrimetallic Complexes of Transition Metals

Christoph Schissler,<sup>[a]</sup> Erik K. Schneider,<sup>[b]</sup> Sergei Lebedkin,<sup>[c]</sup> Patrick Weis,<sup>[b]</sup>  
Gereon Niedner-Schatteburg,<sup>[d]</sup> Manfred M. Kappes,<sup>[b, c]</sup> and Stefan Bräse\*<sup>[a, e]</sup>

**Abstract:** We present a straightforward and generally applicable synthesis route for cofacially linked homo- and heterotrimetallic trisporphyrin complexes. The protocol encompasses synthesising the first aryl-based, trans-*o*-phenylene trisporphyrin starting from pyrrole and benzaldehyde with an overall yield of 3.6%. It also allows investigating the respective *cis*-isomer as the first conformationally restricted planar-chiral trisporphyrin. The free-base ligand was used in subsequent metalation reactions to afford the

corresponding homotrimetallic Mn(III)-, Fe(III)-, Ni(II)-, Cu(II)-, Zn(II)- and Pd(II) complexes – additionally, a small adaptation of the protocol resulted in the defined Ni(II)Fe(III)Ni(II) complex in a total yield of 2.3%. By monitoring Ni(II) insertion into the empty trimeric ligands, we affirmed that the outer porphyrin rings are filled before the internal ring. The molecular species were characterised by <sup>1</sup>H NMR, UV-Vis, photoluminescence, IR, MS, CID, and high-resolution IMS measurements.

## Introduction

The enforced aggregation of various metal ions or prosthetic groups often constitutes an essential instrument in biological systems to arrange catalytically active sites.<sup>[1]</sup> X-ray analysis of the bacterial photosynthetic reaction centre has shown just how sophisticatedly nature has evolved the spatial arrangement of the six interacting tetrapyrroles involved in photosynthesis.<sup>[2]</sup> Among these six chromophores, the primary electron donor in the bacterial and green plant photosynthetic reaction centre consists of a dimeric porphyrinoid pigment, the so-called 'special pair'. This has been studied extensively and is well understood. Complete elucidation of the electron-transport processes subsequent to light triggered charge separation remains one of the fundamental open questions in photosynthesis.<sup>[3]</sup> Inspired by the three-dimensional orientation of bacterial photosynthetic reaction centres in *Rhodospseudomonas viridis*, several porphyrin-based synthetic models have been

developed to investigate catalysts for photosynthetic charge separation and transfer.<sup>[4,5]</sup> Apart from the special pair, one needs to consider an aggregate consisting of at least two additional porphyrins spatially coupled by appropriate prosthetic groups to simulate the charge separation processes occurring in nature.<sup>[3]</sup> A detailed analysis requires tuning distance, orientation and number of discrete chromophores in the model aggregate.<sup>[4]</sup> For this, rigidly fixed geometry and distance are critical – but often difficult to control in artificially synthesised analogues.

Beyond catalysing charge transfer, the chromophore orientation in oligomeric metalloporphyrins can also influence *energy transfer* via corresponding changes to electronic structure and overall photophysical properties. We have been interested in how this can be mediated by cooperative interactions between non-covalently bound porphyrin subunits (and the metal centres contained in them) and have used mass spectrometry (MS) -based methods to study the dependence of electronic

[a] C. Schissler, Prof. S. Bräse  
Institute of Organic Chemistry  
Karlsruhe Institute of Technology (KIT)  
Fritz-Haber-Weg 6, 76131 Karlsruhe (Germany)  
E-mail: braese@kit.edu

[b] E. K. Schneider, Dr. P. Weis, Prof. M. M. Kappes  
Institute of Physical Chemistry  
Karlsruhe Institute of Technology (KIT)  
Fritz-Haber-Weg 2, 76131 Karlsruhe (Germany)

[c] Dr. S. Lebedkin, Prof. M. M. Kappes  
Institute of Nanotechnology  
Karlsruhe Institute of Technology (KIT)  
Hermann-von-Helmholtz-Platz 1, 76344 Eggenstein-Leopoldshafen (Germany)

[d] Prof. G. Niedner-Schatteburg  
Fachbereich Chemie und Forschungszentrum OPTIMAS  
Technische Universität Kaiserslautern  
67663 Kaiserslautern (Germany)

[e] Prof. S. Bräse  
Institute of Biological and Chemical Systems – Functional Molecular  
Systems (IBCS-FMS)  
Karlsruhe Institute of Technology (KIT)  
Hermann-von-Helmholtz-Platz 1, 76344 Eggenstein-Leopoldshafen (Germany)

Supporting information for this article is available on the WWW under <https://doi.org/10.1002/chem.202102376>

This manuscript is part of a Special Issue "Cooperative effects in heterometallic complexes".

© 2021 The Authors. Chemistry - A European Journal published by Wiley-VCH GmbH. This is an open access article under the terms of the Creative Commons Attribution Non-Commercial License, which permits use, distribution and reproduction in any medium, provided the original work is properly cited and is not used for commercial purposes.

structure on the shape of porphyrin dimers containing various metal centres.<sup>[6–8]</sup> In the contexts of both charge and energy transfer in more rigidly fixed geometries, we have begun a systematic study of oligomeric metalloporphyrins covalently linked by way of *o*-phenylene subunits and have recently reported a general synthesis route accessing homo- and heterometallic dimers. Here we present a related synthesis route to access trimetallic trisporphyrins.

In 1982, Wasilewski et al. were the first to synthesise a stacked porphyrin trimer comprising coproporphyrin I doubly-linked via ester bridges. However, due to the  $C_{2h}$  symmetry of the monomeric porphyrin derivatives used, the resulting trimer could only be obtained as an inseparable mixture containing three diastereomers.<sup>[9]</sup> Later on, in the '80s Hamilton et al. and Seta et al. synthesised comparable rather flexible trimeric porphyrins as pigments doubly connected via amide bridges - both to mimic photosynthetic reaction centres and to synthesise molecular wires.<sup>[1,2,10]</sup> Chang et al. modified this multistep, linear-sequence strategy by instead utilising anthracenes as rigid spacers to fix three porphyrins in a defined spatial arrangement. For this, 1,8-anthracene dicarboxaldehydes were used as precursors in a two-fold condensation reaction to afford a triple-decker trisporphyrin.<sup>[11]</sup> Osuka et al. extended this reaction procedure by synthesising 1,3-diphenoxypropane-linked trisporphyrins and was then able to expand the substrate scope to pentameric porphyrin stacks in cooperation with Maruyama.<sup>[4,12]</sup>

The above-mentioned cofacial porphyrin subunits all have at least a 4.94 Å clearance (anthracene case) between the molecular planes.<sup>[11,13]</sup> This can be reduced by exchanging the linker moiety. In the corresponding *o*-phenylene-bridged porphyrin dimer case, the average inter-plane distance reduces to 3.43 Å.<sup>[14]</sup> X-ray analysis confirms that the strong  $\pi$ -interaction of the chromophores can compensate for the 60° bite angle of the *o*-phenylene-linker and yield a cofacial arrangement.<sup>[10]</sup>

In 1992 Osuka et al. developed a step-by-step approach, starting with a cross-condensation reaction, which converts a formyl-substituted porphyrin and a monoprotected phthalaldehyde to a dimeric porphyrin. This was deprotected and utilised in a second cross-condensation reaction to yield the Z-shaped trisporphyrin.<sup>[15]</sup> A complementary synthetic pathway was developed by Therien et al., who transformed the zinc(II) complex of a linear ethynyl-linked alkyl-porphyrin trimer by applying a two-fold transition-metal-mediated [2 + 2 + 2] cycloaddition to yield a Z-shaped trimer.<sup>[16]</sup> To our knowledge, there have been no further synthetic method developments towards cofacially stacked porphyrin trimers since then.

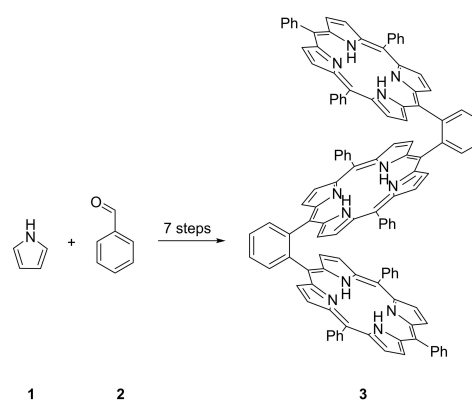
Both pioneering approaches, however, have shortcomings. The procedure of Osuka et al. uses rather expensive bis(3-ethyl-4-methyl-1H-pyrrol-2-yl)methane as the basis for all condensation reactions.<sup>[14]</sup> Additionally, this synthetic approach constrains the fine-tuning of distances because it only allows meso-connected porphyrin subunits and restricts the incorporation of residues.<sup>[17]</sup> Similarly, the synthesis route developed by Therien et al. is not easily applicable to a wide range of different transition metals - in particular, not for heterometallic complexes.<sup>[16]</sup>

Towards this goal, we have aimed in this study for *o*-phenylene linked trisporphyrins as ligands for homo- and heterotrimetallic complexes. We base our approach on our previously reported synthetic protocol for bisporphyrins which we have developed further to access homo- and heterometallic cofacial trisporphyrin complexes in comparatively high yield. We have analysed the molecular structures via NMR spectroscopy in combination with ion mobility spectrometry (IMS). In addition, we report collision-induced dissociation (CID) MS measurements, UV-Vis absorption as well as photoluminescence spectroscopy. Finally, high-resolution MS has been used to evaluate the potential of the prebuilt (free-base) trimeric ligand for selective metal ion complexation from solution.

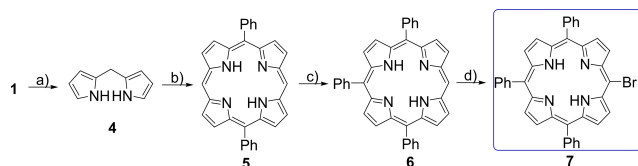
## Results and Discussion

### Homometallic complexes

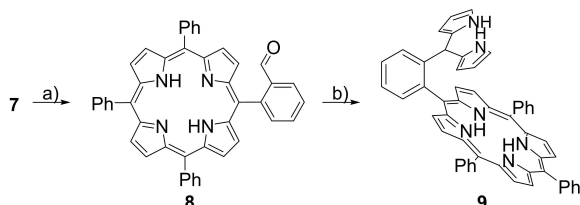
We have developed a facile synthetic route towards the novel *o*-phenylene-trisporphyrin (free base OBTP, 6H-OBTP) **3** as a cofacial ligand system (Scheme 1) using pyrrole and benzaldehyde as starting materials. As previously reported by us for bisporphyrins, we have used the well-established condensation of two pyrroles **1** with paraformaldehyde to yield dipyrromethane **4** in 65% yield to begin the seven-step reaction procedure.<sup>[17,18]</sup> **4** can be used to build up trans-substituted porphyrin cores like 5,15-diphenylporphyrin (**5**) if benzaldehyde is employed as the corresponding aldehyde.<sup>[19]</sup> The subsequent nucleophilic phenylation with PhLi, described by Senge et al. and the following monobromination with NBS, yielded the bromo-porphyrin precursor **7** in an overall yield of 38% (Scheme 2).<sup>[19,20]</sup> After introducing the bromo-substitution, the linker moiety can be incorporated without a second mixed-condensation reaction, as is normally the case in literature.<sup>[17]</sup> Instead, we use a standard Suzuki–Miyaura cross-coupling reaction with 2-formylphenyl-boronic acid as the coupling counterpart (Scheme 3).



**Scheme 1.** Targeted structures: **3**: *o*-phenylene-trisporphyrin (**6H-OBTP**). The porphyrin-based cofacial ligand systems are connected via a phenyl backbone and allows for three-fold coordination of various metal ions.



**Scheme 2.** Synthesis of brominated precursors: a) formaldehyde,  $\text{InCl}_3$ ,  $\text{NaOH}$ ,  $55^\circ\text{C}$ , 3 h, 65%; b) benzaldehyde, TFA, DDQ 4 h, 63%; c)  $\text{PhLi}$ , DDQ, THF,  $0^\circ\text{C} \rightarrow \text{r.t.}$ , 30 min, 95%; d) NBS,  $\text{CH}_2\text{Cl}_2$ ,  $0^\circ\text{C} \rightarrow \text{r.t.}$ , 3 h, 97%.

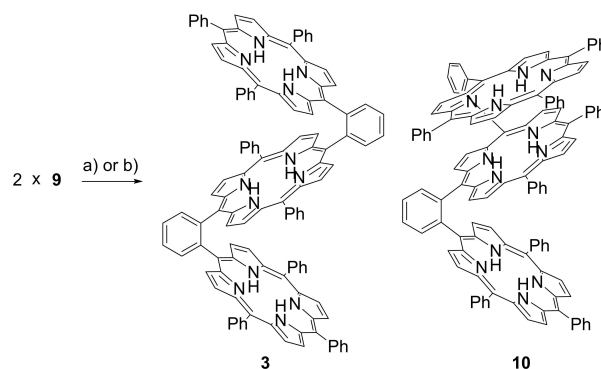


**Scheme 3.** Synthesis of the monomeric porphyrin covalently linked to the phenyl backbone **8** and the subsequent condensation reaction to **9** bearing dipyrromethane as part of the future internal diphenyl-porphyrin. a) 2-formylphenyl-boronic acid,  $\text{Pd}(\text{PPh}_3)_4$ ,  $\text{K}_3\text{PO}_4$ , THF,  $80^\circ\text{C}$ , 14 h, 78%; b) pyrrole, TFA,  $\text{NEt}_3$ , r.t., 4 h 93%.

Rather than reacting the aldehyde functionalities by mixed condensation to obtain the respective *o*-phenylene-bisporphyrin, as previously reported by us, we have instead converted them to a porphyrin-bearing dipyrromethane **9**. First, we attempted Bein's strategy, which has been employed to synthesise di(1H-pyrrole-2-yl)methane (**4**) using  $\text{InCl}_3$  as Lewis acid and  $\text{NaOH}$  as a neutralising agent. We could detect the desired product via MS but only as a side product besides the oxidised dipyrromethane. In the second attempt, we explored TFA as a catalyst alongside  $\text{NEt}_3$  as a base - a procedure closer to commonly used conditions in porphyrin chemistry. After 4 h stirring at room temperature and continuously adding TFA, we obtained the 5-(2-(di(1H-pyrrol-2-yl)methyl)phenyl)-10,15,20-triphenylporphyrin (**9**) in 93% isolated yield after performing flash-chromatography on silica gel and eluting with toluene. The corresponding NMR spectra were recorded in toluene- $d_8$  to avoid oxidation and show the nine dipyrromethane protons in the expected region of 4.98–6.30 ppm.

Additionally, the porphyrin NH signals experience a downfield shift to  $-2.19$  ppm due to additional deshielding from the pyrrole subunits. This robust procedure provides monomeric porphyrin precursors in an excellent total yield of 28% via 6 steps. The dipyrromethane subunit now takes part in an acid-catalysed concluding condensation with benzaldehyde in a ratio of 1:1, as represented in Scheme 4. Surprisingly we noticed by-product **10** in approaches a) and b), which could not be separated from **3** even after four consecutive flash column chromatography passes on silica gel eluting with differing solvents.

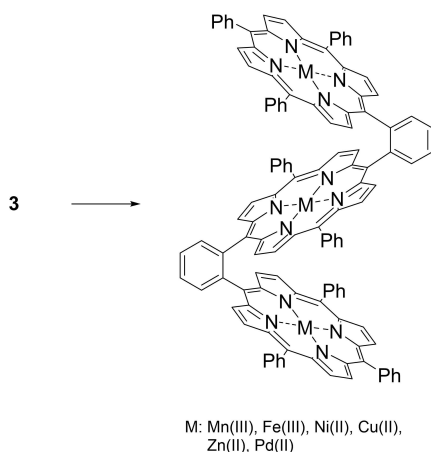
Additionally, mass spectrometry alone did not help to solve the corresponding molecular structure since the **3** and **10** are isomers. Since we additionally obtained *o*-phenylene-bisporphyrin in traces, it became clear that scrambling plays a role in



**Scheme 4.** Condensation reaction of two dipyrromethane-containing porphyrins with benzaldehyde yielding two possible isomers of trimeric porphyrin stacks: *trans*-isomer **3** and *cis*-isomer **10**. a) benzaldehyde (7.22 equiv.), TFA (8.46 equiv.), DDQ (2.10 equiv.),  $\text{NEt}_3$ ,  $\text{CH}_2\text{Cl}_2$ , r.t. 26.5 h, 13%; b) benzaldehyde (2.00 equiv.),  $\text{BF}_3 \cdot \text{OEt}_2$  (2.00 equiv.), DDQ (2.44 equiv.),  $\text{NEt}_3$ ,  $\text{CH}_2\text{Cl}_2$ , r.t. 19 h, 1.9%

this condensation reaction. Subsequent IMS of the singly protonated trimers proved the identity and additional presence of the *cis*-isomer. From the integrated mobilograms, we could determine the *trans*:*cis* ratio to be 25:1 with TFA and 21:(8 + 1) with  $\text{BF}_3 \cdot \text{OEt}_2$  as catalyst (see IMS section for details). By contrast, the  $^1\text{H}$  NMR spectra show the ratio of the neutral molecules to be 50:1 or 5:1, respectively. The IMS data overestimate the *cis*/*trans*-ratio probably due to the higher basicity of the *cis*-isomer and, therefore, higher ionizability via protonation. *Cis*-*o*-phenylene-trisporphyrin is the first conformationally restricted planar chiral porphyrin trimer reported in the literature, and its formation can be enhanced by choosing  $\text{BF}_3 \cdot \text{OEt}_2$  as a catalyst. DFT calculations show an energy gap of only 0.14 eV between the *trans*- and the *cis* isomer underlining that the isomeric ratio of the condensation reaction is kinetically controlled (see DFT calculation (Supporting Information) for details). Since the TFA catalysed reaction showed less scrambling whereas the overall yield (13%) is superior, we optimised the reaction procedure by consequently adding the minimum amount of benzaldehyde necessary to see a conversion while retaining a rather high concentration of the acid in previously degassed  $\text{CH}_2\text{Cl}_2$ . *trans*-6H-OBTP contains a two-fold axis as a symmetry element which leads to rather simple NMR spectra. Notably, are the downfield shifted NH protons occurring at  $-3.79$  ppm as a broad signal for the outer four NH protons and at  $-4.20$  ppm as a comparatively sharp singlet for the two inner NH protons. In conclusion, our novel synthetic route presents the synthesis of 5,15-bis(2-(10,15,20)-triphenylporphyrinyl)phenyl)-10,20-diphenylporphyrin (**3**) the first aryl-based trimeric porphyrin stack, which can be synthesised starting with pyrrole and benzaldehyde over 7 steps in an overall yield of 3.6%.

Next, the as-synthesised free-base ligand with the *trans*/*cis* ratio of 98:2 was triply metallated with six different transition metals (Scheme 5), and the resulting metal complexes, bearing the same *trans*/*cis* ratio were systematically analysed with UV-Vis, IR-spectroscopy, MS and IMS. For the metal coordination, we observed that reaction times needed to be only slightly



**Scheme 5.** Cofacial porphyrin-based homotrimeric complexes a) (11) <sup>+</sup>Mn(III): MnCl<sub>2</sub>, DMF, 150 °C, 3 h, 86%; (12) <sup>2+</sup>Fe(III): FeBr<sub>2</sub>, HCl, DMF, 140 °C, 3 h, 89%; (13) Ni(II): Ni(OAc)<sub>2</sub> × 4 H<sub>2</sub>O, CHCl<sub>3</sub>/MeOH, 100 °C, 17 h; 95%; (14) Cu(II): Cu(OAc)<sub>2</sub>, CHCl<sub>3</sub>/MeOH, 80 °C, 3 h, 65%; (15) Zn(II): Zn(OAc)<sub>2</sub>, CHCl<sub>3</sub>/MeOH, r.t., 2 h, 86%; (16) Pd(II): Pd(OAc)<sub>2</sub>, CHCl<sub>3</sub>/MeOH, 80 °C, 2 h, 84%; \* 3Ni-, 3Cu-, 3Zn- and 3Pd-OBTP have been detected as monocations by MS, whereas 3Fe-OBTP has been detected with adducts of O and Cl. The Mn-trimer was observed with mainly two attached chlorides.

extended relative to our previous dimer work to obtain complete three-fold complexation.<sup>[17]</sup> Exceptionally this does not hold for the 3Ni-OBTP 13 complex since we observed degradation while stirring in DMF at 100 °C.

Additionally, we measured the CID spectra of two differently synthesised [2Ni-3H-OBTP]<sup>+</sup> complexes. In the first approach, the ligand was only partially filled with Ni(II) by sampling at 50% of the reaction time required for complete filling with three metals. In the second approach, the Ni(II)porphyrin 18 (see below) was coupled to form a trimer. The CID-spectra have been measured using a Bruker timsTOF system which couples high-resolution ion mobility spectrometry with mass spectrometry (IMS-MS). The fragment spectra of both samples look almost identical and can be found in the Supporting Information.

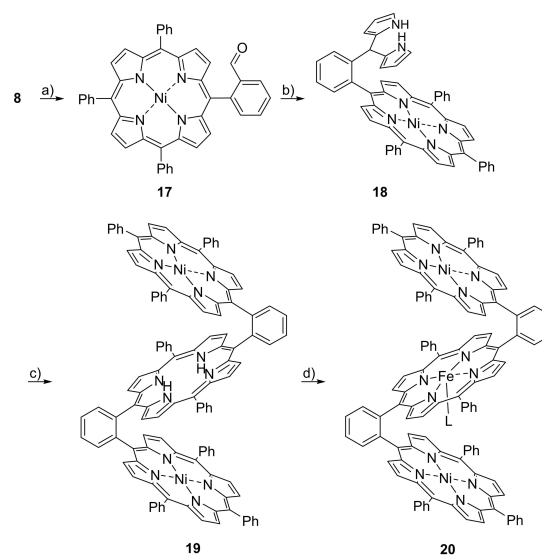
They do not show fragments corresponding to protonated free-base monomers. Instead, nickelated monomers, as well as 1.5-mers containing one nickel atom and residues of a second porphyrin ring, are observed as main products. This and the similarities between the two sets of CID-spectra allow us to conclude that both approaches lead to the same main product: Ni has inserted into each of the two outer porphyrins exclusively. We, therefore, agree with Osuka et al., who postulated in 1991 that the outer porphyrin subunits were metalated first.<sup>[14]</sup>

### Heterometallic complexes

As a proof of principle, to realise porphyrin-based-transition-metal-containing trimeric heterometallic complexes, we specifically built a trisporphyrin containing two Ni(II) and one Fe(III) centre – which may also be thought of as an extended carbon

monoxide dehydrogenase active site analogue. To circumvent potential oxidation of the porphyrin-dipyrromethane 9, the Ni(II) cation was inserted after the Suzuki-Miyaura cross-coupling reaction in the monomeric formyl-phenyl-porphyrin 8 by treatment with Ni(OAc)<sub>2</sub> × 4 H<sub>2</sub>O at 100 °C for 18.5 h in 93% yield (Scheme 6). The conversion of the aldehyde functionality to the dipyrromethane-containing Ni(II)porphyrin 18 was conducted as described for the free-base analogue by doubling the reaction time resulting in a yield of 84%. Apart from the missing porphyrinic NH protons and slightly increased coupling constants (from <sup>3</sup>J=4.7 Hz to 4.9 Hz), Ni(II) coordination leads to the sharpening of the signals arising from the dipyrromethane subunit in the <sup>1</sup>H NMR spectrum. A possible interpretation is that Ni(II) complexation prevents intramolecular hydrogen bonding, which would otherwise occur in the free-base analogue 9. In a subsequently performed condensation reaction, similar to Scheme 5 but with reduced reaction time, the 2Ni-2H-OBTP, 19, can be obtained in 14% yield. To isolate the 2Ni-2H-OBTP species, a tedious work-up comprising three consecutive flash-column chromatographic cycles with differing solvents was necessary. The ring currents of the two adjacent porphyrins arranging in a sandwich-like structure lead to a significant up-field shift of the NH protons of the interior porphyrin ring to –5.01 ppm. This indicates a significant change in the electronic nature of this molecular subunit in comparison to the free-base porphyrin contained in the Ni-2H-o-phenylene-bisporphyrin - as reported earlier by our consortium.<sup>[17]</sup>

This observation also led us to look more closely at the reaction process leading to three-fold Ni(II) complexation of the empty trisporphyrin ligand. Indeed, the reaction time depend-



**Scheme 6.** Synthetic route towards an extended artificial carbon monoxide dehydrogenase active site analogue (20) as proof of principle reaction for several trimeric heterometallic porphyrin complexes. a) Ni(OAc)<sub>2</sub> × 4 H<sub>2</sub>O, CHCl<sub>3</sub>, MeOH, 100 °C, 18.5 h, 93% b) pyrrole, TFA, NEt<sub>3</sub>, r.t., 8 h, 84%, c) benzaldehyde (2,16 equiv.), TFA (3.69 equiv.), NEt<sub>3</sub>, CH<sub>2</sub>Cl<sub>2</sub>, r.t., 3 h, 14%, d) FeBr<sub>2</sub>, DMF, 150 °C, 2 h, 94%. (Ligand L cannot be determined precisely as in MS we could assign adducts with several oxygens as dominant counter ions).

ence of the  $^1\text{H}$  NMR signal at  $-5.01$  ppm provided further proof for the metalation sequence inferred from the CID measurements. As an aside: it also shows that the two external Ni(II) containing porphyrins in spatial proximity to an initially empty central site can cooperatively influence its electronic properties and thus also the electronic properties of the third metal centre.

The interior free-base porphyrin can undergo a reaction with  $\text{FeBr}_2$  in DMF at  $150^\circ\text{C}$  for 2 h to coordinate Fe(III) as the third cation in 74% yield to afford a species bearing two Ni(II) and one Fe(III) -centre, **20**. The Fe-2Ni-OBTP represents the first trimeric heterometallic porphyrin complex which can be obtained in a total yield of 2.3% beginning with pyrrole and benzaldehyde as starting material and underlines the robustness of the presented synthetic protocol.

Based on the results shown, one can assume this methodology to be suitable for another analogous homo- and heterometallic porphyrin complexes. By simply using two different dipyrromethane-bearing porphyrins in a mixed condensation reaction in the presence of an aldehyde and subsequent metal insertion, one could, in principle, synthesise all 18 distinguishable perturbative combinations of three different metals (taking point symmetry into account for the *trans* isomer). In the case of different *meso*-substitutions of the dipyrromethane-containing porphyrins, 27 combinations would result due to broken point symmetry. Magnetism/spintronics, catalysis and optical sensors are several fields for which such compounds may be of applications interest.

### Ion mobility data

The complexes presented in this work have been characterised by NMR-, UV-Vis- IR-spectroscopy and MS, but due to crystallisation problems, their 3D structure could not be established by X-Ray diffraction.

Relative to the signature expected for purely the *trans* isomer, the NMR-spectra of the 6H-OBTP showed some additional (weaker) lines. To check whether these could be explained by the simultaneous presence of the *cis*-isomer as shown in Scheme 3, we also performed IMS-MS measurements.<sup>[17]</sup> This yields mobilograms (for a given mass-to-charge selected ion). Multi-peaked mobilograms reflect isomers with different collision cross-sections ( $^{\text{TIMS}}\text{CCS}_{\text{N}_2}$ ) resolved by transiting an inert  $\text{N}_2$  collision gas. Figure 1 shows the mobilograms of  $[\text{7H-OBTP}]^+$  synthesised by the two routes a) and b) as indicated in Scheme 4. The corresponding mass spectra can be found in the Supporting Information.

As can be seen in Figure 1, the molecules synthesised by route a) and b) show two or three different peaks in their respective mobilograms – indicating the presence of multiple (separable) isomeric forms. It is easy to imagine at least four different isomers, namely *cis*- and *trans*- $[\text{7H-OBTP}]^+$ , each with their two different corresponding protonation isomers (protomers). Either the inner porphyrin or one of the two outer porphyrins could be protonated. For both syntheses, peak III is

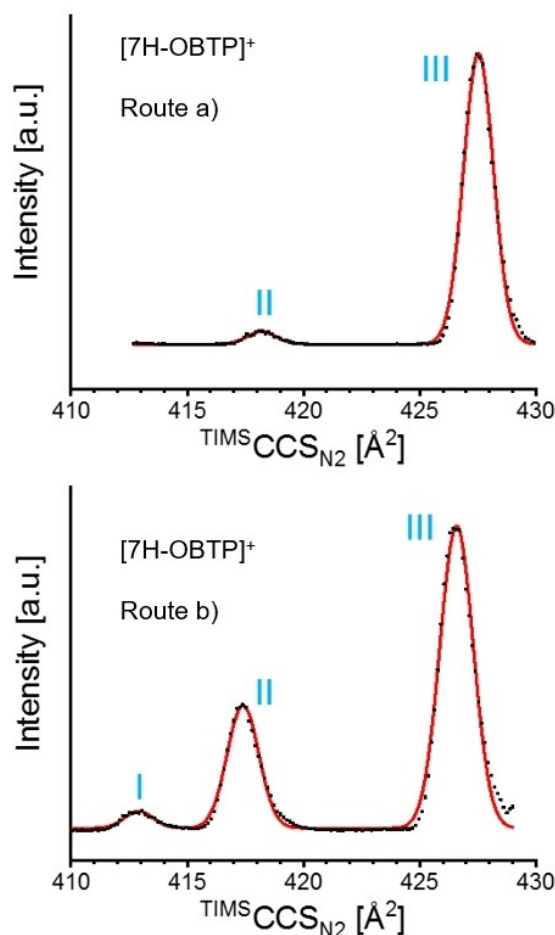


**Figure 1.** High-resolution ion mobility measurements (IMS) of singly protonated, free base OBTP electrospayed from a 0.2 mM solution of DCM and DMF (80:20). The mobilograms of  $[\text{7H-OBTP}]^+$  from the products of synthetic routes a) and b) in Scheme 3 show up to three resolvable isomers (I–III). Route a) produces smaller relative amounts of isomer II than route b), whereas isomer I cannot be obtained by route (a). Isomer III is the main product in both cases. The exact peak position of the isomers for the two synthetic routes vary due to statistical errors, which we estimate to be 0.5% (ca.  $2 \text{ \AA}^2$ ) between different runs.

found to be the dominant peak, we attribute it to the *trans* isomer by our interpretation of the NMR measurements.

This leads to the conclusion that peaks II and I correspond to the *cis* isomer, probably in different kinetically locked rotamer or protomer forms. The varying intensities of peak II and the non-existence of peak I in synthetic route a) indicate that the two catalysts used for the respective reactions yield different amounts of the *cis* isomer. Hence, it is conceivable that there may also be catalysts that would form the *cis* isomer as the main product. In future work, it will be of interest to explore this further.

### Absorption and fluorescence spectra

It is well known that in solution, porphyrins display several sharp, intense and characteristic bands in their electronic

absorption spectra. Figure 2 compares the absorption of 6H-OBTP (3), 3Pd-OBTP complex (16) and Fe-2Ni-OBTP-4O (20) dissolved in  $\text{CH}_2\text{Cl}_2$  with that of the parent monomeric forms, i.e. of free-base tetraphenyl porphyrin (2H-TPP) and its Pd(II) derivative Pd-TTP. The absorption spectra of the latter monomeric compounds correspond well to the literature. The extinction of the sharp Soret band (SB) of 2H-TTP at 417 nm and Pd-TTP at 416 nm were determined as  $\epsilon(\text{SB})=4.68 \times 10^5$  and  $3.24 \times 10^5 \text{ M}^{-1}\text{cm}^{-1}$ , respectively. This band notably broadens and blueshifts to 404 nm in OBTP and 406 nm in both trimetallic trisporphyrins. The broadening only partly explains the decrease of extinction in the free-base OBTP trimer (6H-OBTP,  $\epsilon(\text{SB})=3.11 \times 10^5 \text{ M}^{-1}\text{cm}^{-1}$ ) vs. monomer (2H-TTP): their Soret band area ratio is about 2:1, not 3:1. Such reduction of the SB oscillator strength has also been observed in dimeric porphyrin cages and interpreted as a signature of strong electronic coupling between monomeric chromophore units.<sup>[21]</sup> This effect is even more pronounced in the trimetallic vs. monometallic (Pd-TTP) complexes:  $\epsilon(\text{SB})=0.73 \times 10^5$  and  $0.90 \times 10^5 \text{ M}^{-1}\text{cm}^{-1}$  in 3Pd-OBTP and Fe-2Ni-OBTP, respectively, and the SB area ratio of 3Pd-OBTP vs. Pd-TTP is only  $\sim 0.6:1$ . In contrast to the Soret band, the Q-band in the green-red spectral region (with four distinct components observed for the free-base monomer and trimer) displays a moderate redshift in the trimeric porphyrins, for example, from 523 nm in Pd-TTP to 532 nm in 3Pd-OBTP. A quantitative comparison of the Q-band oscillator strengths was hindered by band broadening and tailing in the spectra of the trimeric porphyrins and was not done. We also recorded photoluminescence spectra of the corresponding air saturated solutions. Similar to 2H-TTP, the free-base OBTP trimer emits moderately intense red

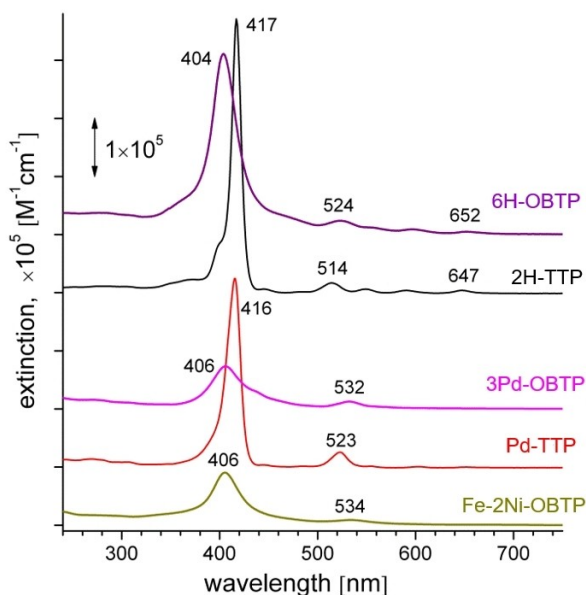


**Figure 2.** Absorption spectra (vertically shifted for clarity) of trimeric 6H-OBTP (3), 3Pd-OBTP (16) and Fe-2Ni-OBTP (20) relative to monomeric 2H-TTP and Pd-TTP in dichloromethane solutions. Sample concentrations are within the 5–20  $\mu\text{M}$  range. The numbers indicate the positions of the absorption band maxima.

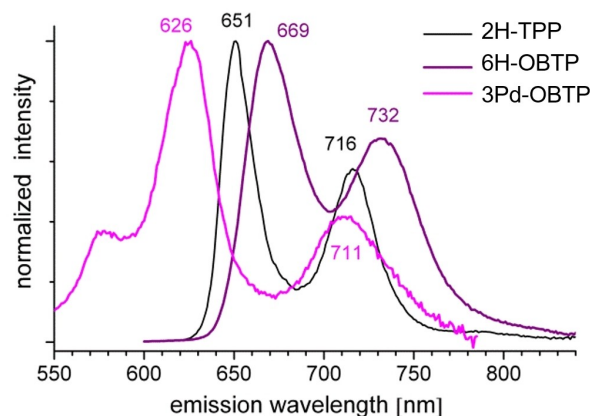


**Figure 3.** Normalised fluorescence spectra of 6H-OBTP (3) and 3Pd-OBTP (16) relative to monomeric 2H-TTP in dichloromethane solutions. The excitation wavelengths correspond to the respective positions of the Soret band maxima (see Figure 2).

fluorescence (Figure 3). The major and vibronic emission bands of 6H-OBTP at 669 and 732 nm are slightly redshifted and notably broadened in comparison to 2H-TTP. The fluorescence intensity moderately decreases in the trimer as referred to the monomer: the emission quantum yield,  $\Phi_{\text{FL}}$  was determined as 0.022 and 0.047, respectively.

For comparison, Figure 3 also shows the spectrum of weak fluorescence ( $\Phi_{\text{FL}} \ll 0.001$ ) of 3Pd-OBTP. The parent monomer Pd-TTP emits similarly weak fluorescence (not shown), which peaks at about 610 nm, in agreement with the first observation by Gouterman et al.<sup>[22]</sup> At higher wavelengths, however, this fluorescence was strongly dominated by a residual impurity of 2H-TTP ( $\sim 1\%$ ) in the sample of Pd-TTP. Finally, practically no emission could be detected for Fe-2Ni-OBTP, in agreement with previous observations for other Ni(II)-containing porphyrins.<sup>[23]</sup>

## Conclusion

We present a straightforward new synthesis route for homo- and heterotrimetallic trisporphyrin complexes. The developed protocol makes use of the first aryl-based *trans*-*o*-phenylene trisporphyrin, which we have prepared in an overall yield of 3.6% over 7 steps starting with pyrrole and benzaldehyde. The synthesis also allows us to investigate the respective *cis*-isomer as the first conformationally restricted planar-chiral trisporphyrin. The *o*-phenylene linked free-base trisporphyrin ligand was used as the basis to synthesise the homotrimetallic Mn(III)-, Fe(III)-, Ni(II)-, Cu(II)-, Zn(II)- and Pd(II)- complexes. Using an analogous procedure, we have also prepared the defined Ni(II) Fe(III)Ni(II)- heterometallic complex in a total yield of 2.3% (beginning with pyrrole and benzaldehyde), thus underscoring the robustness of our synthetic protocol. The molecular species were characterised by  $^1\text{H}$  NMR, UV-Vis, luminescence, IR, MS, CID and high-resolution IMS measurements. Probes of Ni(II) insertion kinetics suggest that it is possible to control the metalation order – also by way of the characteristic electronic environment of the central porphyrin ring. Correspondingly, we

are exploring the uses of the ligand as a selective complexation probe for dissolved metal ions.

## Experimental Section

The synthetic procedures of all compounds are included in to the Supporting Information.

## Acknowledgements

We thank S. Notter, S. Jaschik, F. Bösch and S. Marschner for their help in conducting synthesis of the precursors. C.S. gratefully acknowledges the Fonds der Chemischen Industrie (FCI) and the graduate program of the federal state of Baden-Württemberg (LGF) for financial support. SB also thanks to the Collaborative Research Center TRR 88 “3MET” and the Deutsche Forschungsgemeinschaft (DFG, German Research Foundation) for support through project B2. Additionally, S.B. acknowledges support under Germany’s Excellence Strategy via the Excellence Cluster 3D Matter Made to Order (EXC-2082/1–390761711). E.K.S., P.W., G.N.S. and M.M.K. gratefully acknowledge support by the Deutsche Forschungsgemeinschaft (DFG) as administered by the Collaborative Research Center TRR 88 “3MET” through project C6. M.M.K. thanks KIT for funding of the TIMS-TOFMS used in this study. Open Access funding enabled and organized by Projekt DEAL.

## Conflict of Interest

The authors declare no conflict of interest.

**Keywords:** active site analogue · carbon monoxide dehydrogenase · cofacial · heterotrimetallic · homotrimetallic · ion mobility spectrometry · porphyrin trimers

- [1] G. M. Dubowchik, A. D. Hamilton, *J. Chem. Soc. Chem. Commun.* **1987**, 293–295.
- [2] G. M. Dubowchik, A. D. Hamilton, *J. Chem. Soc. Chem. Commun.* **1986**, 1391–1394.
- [3] I. Abdalmuhdi, C. Chang, *J. Org. Chem.* **1985**, *50*, 411–413.
- [4] T. Nagata, A. Osuka and K. Maruyama, *J. Am. Chem. Soc.* **1990**, *112*, 3054–3059.
- [5] M. R. Wasielewski, *Chem. Rev.* **1992**, *92*, 435–461.
- [6] K. Brendle, U. Schwarz, P. Jäger, P. Weis, M. Kappes, *J. Phys. Chem. A* **2016**, *120*, 8716–8724.
- [7] E. Schneider, K. Brendle, P. Jäger, P. Weis, M. M. Kappes, *J. Am. Soc. Mass. Spec.* **2018**, *29*, 1431–1441.
- [8] P. Jäger, K. Brendle, E. Schneider, S. Kohaut, M. K. Armbruster, K. Fink, P. Weis, M. M. Kappes, *J. Phys. Chem. A* **2018**, *122*, 2974–2982.
- [9] M. R. Wasielewski, M. P. Niemczyk, W. A. Svec, *Tetrahedron Lett.* **1982**, *23*, 3215–3218.
- [10] P. Seta, E. Bienvenue, P. Maillard, M. Momenteau, *Photochem. Photobiol.* **1989**, *49*, 537–543.
- [11] C. Chang, I. Abdalmuhdi, *J. Org. Chem.* **1983**, *48*, 5388–5390.
- [12] A. Osuka, F. Kobayashi, K. Maruyama, *Bull. Chem. Soc. Jpn.* **1991**, *64*, 1213–1225.
- [13] J.-M. Camus, P. D. Harvey, R. Guillard, *Macroheterocycles* **2013**, *6*, 13–22.
- [14] A. Osuka, S. Nakajima, T. Nagata, K. Maruyama, K. Toriumi, *Angew. Chem. Int. Ed.* **1991**, *30*, 582–584.
- [15] A. Osuka, S. Nakajima, K. Maruyama, *J. Org. Chem.* **1992**, *57*, 7355–7359.
- [16] J. T. Fletcher, M. J. Therien, *J. Am. Chem. Soc.* **2000**, *122*, 12393–12394.
- [17] C. Schissler, E. K. Schneider, B. Felker, P. Weis, M. Nieger, M. M. Kappes, S. Bräse, *Chem. - Eur. J.* **2021**, *27*, 3047–3054.
- [18] M. Calik, F. Auras, L. M. Salonen, K. Bader, I. Grill, M. Handloser, D. D. Medina, M. Dogru, F. Löbermann, D. Trauner, *J. Am. Chem. Soc.* **2014**, *136*, 17802–17807.
- [19] D. C. Götz, T. Bruhn, M. O. Senge, G. Bringmann, *J. Org. Chem.* **2009**, *74*, 8005–8020.
- [20] M. O. Senge, W. W. Kalisch, I. Bischoff, *Chem. - Eur. J.* **2000**, *6*, 2721–2738.
- [21] L. Zanetti-Polzi, A. Amadei, R. Djemili, S. p. Durot, L. Schoepff, V. r. Heitz, B. Ventura, I. Daidone, *J. Phys. Chem. C* **2019**, *123*, 13094–13103.
- [22] J. B. Callis, M. Gouterman, Y. Jones, B. Henderson, *J. Mol. Spectrosc.* **1971**, *39*, 410–420.
- [23] A. Antipas, M. Gouterman, *J. Am. Chem. Soc.* **1983**, *105*, 4896–4901.

Manuscript received: July 1, 2021

Version of record online: August 20, 2021